Article

Experimental Study on Mechanical Properties and Fractal Dimension of Pore Structure of Basalt–Polypropylene Fiber-Reinforced Concrete

Ditao Niu [1,2,*], Daguan Huang [2], Hao Zheng [2], Li Su [2], Qiang Fu [2,*] and Daming Luo [2]

[1] State Key Laboratory of Green Building in Western China, Xi'an University of Architecture & Technology, Xi'an 710055, China

[2] College of Civil Engineering, Xi'an University of Architecture & Technology, Xi'an 710055, China; hdg0505@163.com (D.H.); niurougan522@163.com (H.Z.); suli9290@outlook.com (L.S.); dmluo@xauat.edu.cn (D.L.)

* Correspondence: niuditao@163.com (D.N.); fuqiangcsu@163.com (Q.F.)

check for updates

Abstract: This study investigates the effects of basalt–polypropylene fibers on the compressive strength and splitting tensile strength of concrete and calculates the fractal dimension of the pore structure of concrete by using a fractal model based on the optical method. Test results reveal that hybrid fibers can improve the compressive strength and splitting tensile strength of concrete, and the synergistic effect of the hybrid fibers is strongest when the contents of basalt fiber (BF) and polypropylene fiber (PF) are 0.05% each, and that the maximum increments in compressive strength and splitting tensile strength are 5.06% and 9.56%, respectively. The effect of hybrid fibers on splitting tensile strength is greater than on compressive strength. However, hybrid fibers have adverse effects on mechanical properties when the fiber content is too high. The pore structure of basalt–polypropylene fiber-reinforced concrete (BPFRC) exhibits obvious fractal characteristics, and the fractal dimension is calculated to be in the range of 2.297–2.482. The fractal dimension has a strong correlation with the air content and spacing factor: the air content decreases significantly whereas the spacing factor increases with increasing fractal dimension. In addition, the fractal dimension also has a strong positive correlation with compressive strength and splitting tensile strength. Therefore, the fractal dimension of the pore structure can be used to evaluate the microscopic pore structure of concrete and can also reflect the influence of the complexity of the pore structure on the macroscopic mechanical properties of concrete.

Keywords: basalt fiber; polypropylene fiber; hybrid fiber-reinforced concrete; mechanical properties; pore structure; fractal dimension

1. Introduction

Concrete is widely used in engineering structures because of its low cost, simplicity of preparation, and excellent strength [1]. However, concrete also has disadvantages such as a low tensile strength, poor toughness, and high brittleness, which adversely affect the safety, applicability, and durability of the concrete structure [2]. Many studies have shown that the mechanical properties and durability of concrete can be effectively improved by incorporating fibers into it, thus obtaining fiber-reinforced concrete for high strength, toughness, and durability [3,4].

Fibers can be incorporated into concrete in two ways: incorporation of a single type of fiber, and incorporation of fibers of different types or sizes. Incorporation of a single type of fiber provides limited improvement in concrete performance. When hybrid fibers obtained by mixing fibers of different types or sizes are incorporated into concrete, the hybrid fibers can induce their respective reinforcing effects

in different layers and stress stages of concrete, and consequently, the improvement in the concrete performance is more remarkable [5]. Steel–polypropylene fiber-reinforced concrete is currently the most widely used hybrid fiber-reinforced concrete. The elastic modulus and strength of steel fiber (SF) are high, because of which its incorporation into concrete can effectively reduce the brittleness of concrete, and improve its mechanical properties and load-bearing capacity. Polypropylene fiber (PF) has a low elastic modulus and good ductility; as a result, its incorporation into concrete can effectively improve the splitting tensile strength and flexural strength of concrete [6,7]. Badogiannis et al. reported that SF and PF could significantly improve the mechanical properties of pumice concrete and that the maximum increments in the compressive strength and splitting tensile strength were 76% and 110%, respectively [8]. Pajak et al. studied the flexural properties of steel–polypropylene fiber-reinforced concrete and found that the hybrid fibers could effectively improve the mechanical properties and toughness of concrete [9]. Aslani et al. demonstrated that the compressive strength and elasticity modulus of steel–polypropylene fiber-reinforced concrete were higher than those of SF-reinforced concrete and PF-reinforced concrete [10]. However, the chemical composition of SF is the same as that of reinforcing bars; because of this, SF rusts easily in a corrosive environment, which limits the application scope of steel–polypropylene fiber-reinforced concrete [11].

Basalt fiber (BF) is made from basalt as raw material via melting and drawing at high temperatures. BF has advantages such as a high tensile strength, high-temperature resistance, corrosion resistance, and a high elastic modulus. Moreover, it is a type of a green, environmentally-friendly fiber and a good substitute for SF [12,13]. Therefore, basalt–polypropylene fiber-reinforced concrete (BPFRC)—prepared by mixing BF instead of SF with PF—has a wider application range. The mechanical properties of BPFRC have been preliminarily studied by some researchers. Ghazy et al. reported that compressive strength improved significantly when it was incorporated with BPFRC composed of 0.1% BF and 0.1% PF [4]. Wang et al. demonstrated that when the BF and PF contents were 0.15% and 0.033%, respectively, the compressive strength and splitting tensile strength of concrete increased by 14.1% and 48.6%, respectively [14]. Kong et al. investigated the mechanical properties of basalt–polypropylene hybrid fiber-reinforced recycled concrete under high-temperature conditions [15]. They showed that the compressive strength and splitting tensile strength of concrete reinforced with hybrid fibers were higher than those of plain concrete. However, several other studies showed that incorporation of hybrid fibers composed of BF and PF improved the splitting tensile strength of concrete, but lowered its compressive strength [16,17].

3D printing techniques have developed rapidly and been introduced to the field of civil engineering structures. Rapid development of the technique in the construction field depends on the development of high-performance cementitious materials compatible with 3D printers [18]. Some studies have shown that the addition of fibers in the preparation of 3D printing cementitious materials can improve structural performance [19]. Hambach et al. found that when fibers were aligned along the printing path, the flexural strength of the printed structure in the designated direction increases significantly [20]. Panda et al. reported that when the glass fiber content was 1%, the flexural and tensile strength of the printed specimens improved significantly and in an obvious directional dependency, but there was little effect on compressive strength [21]. Ma et al. demonstrated that a cementitious composite containing 0.5% basalt fibers had favorable printability and mechanical properties, and the 3D-printed samples performed obviously mechanical anisotropy [22]. The research on the anisotropic mechanics of 3D-printed fiber-reinforced materials is not adequately comprehensive. Therefore, more experiments should be carried out to promote the practical application of 3D printing techniques in the field of construction.

The structure of composites includes two characteristic scales: macroscopic and microscopic. The macroscopic mechanical behavior of composites is affected by the volume fraction, shape and distribution of the components. Researchers have proposed many mathematical techniques to solve this interaction problem. The common methods include the Self-Consistent Method [23], Generalized Self-Consistent Method [24], Mori–Tanaka Method [25], Asymptotic Homogenization Method [26],

and so on. The Asymptotic Homogenization Theory has developed into the main method to solve the equivalent mechanical properties of composite materials in recent years. By establishing the asymptotic displacement field that depends on the change of two-scale coordinate variables, the governing equation reflecting the microstructure is derived, and the average material properties are obtained [27]. The pore structure of concrete is an important aspect of its microstructure, which directly affects mechanical properties, frost resistance, and other macroscopic properties of concrete. Because of the increasing complexity of high-performance concrete, conventional parameters cannot effectively describe the complexity of the pore structure quantitatively, which hinders the study of the relationship between the pore structure and the macroscopic properties of concrete [28]. Fractal theory, as a new approach for describing the complexity and irregularity of matter, has been introduced and gradually applied to the study of pore structure, wherein it quantifies the complexity of the micropore structure as a fractal dimension. The relationship between the microstructure and macroscopic properties of concrete can be studied by utilizing the fractal dimension. In recent years, with advances in research, fractal models of multiple pore structures based on various pore structure characterization methods have been established, and the relationship between fractal dimension and macroscopic performance has been discussed [29–31]. Jin et al. established a model of the relationship between the fractal dimension and compressive strength. Their results revealed that the fractal dimension could well-characterize the relationship between the micropore structure and the macroscopic mechanical properties [30]. Cui et al. revealed that the fractal dimension obtained by a thermodynamics method could describe the pore size distribution of concrete better than that obtained using the Menger sponge model, and that there was a strong positive correlation between the mechanical properties of concrete and the fractal dimension [31]. Zhao et al. calculated the fractal dimension of BF-reinforced concrete by using a fractal model based on an optical method; their results revealed that with an increasing fractal dimension, compressive strength increased and air content decreased [32]. Yu et al. tested the pore structure and mechanical properties of perlite cement stone, but their results revealed that with an increasing fractal dimension, compressive strength decreased and porosity increased [33]. This finding is consistent with the results reported in other literature [34].

From a review of the aforementioned studies, it is clear that research conducted on the mechanical properties of BPFRC is not comprehensive enough and that the research conclusions are insufficiently unified, which hinders the application and development of BPFRC to a certain extent. Because of the different testing methods of the pore structure and different interpretations of the physical meaning of the fractal dimension, there is a large gap in existing research results. Research on the pore structure of concrete and its mechanical properties needs to be improved. Therefore, it is necessary to further study the fractal characteristics of the pore structure. The main objective of this work is to investigate the mechanical properties of concrete reinforced with basalt–polypropylene hybrid fibers and to determine the optimal contents of BF and PF in order to significantly improve the compressive strength and splitting tensile strength of concrete. The fractal dimension of the pore structure is calculated using a fractal model based on an optical method. In addition, the relationship of the fractal dimension with the mechanical properties of concrete and other parameters of the pore structure is also investigated.

2. Materials and Test Methods

2.1. Materials

P.O 42.5R Portland cement (OPC), granulated blast furnace slag powder (BFS), silica fume (SF) and fly ash (FA) were used to prepare test specimens. The physical properties and chemical composition of the cementitious material are listed in Table 1. BF and PF are shown in Figure 1a,b, respectively, and their physical and mechanical properties are listed in Table 2. The coarse aggregate (CA), with 5–20 mm continuous gradation, consisted of gravel sourced from the Shaanxi Jingyang mountain. The fine aggregate (S) used was medium sand with a fineness modulus of 2.8. Tap water (W) was used for mixing. A polycarboxylate superplasticizer (PBS) was used to achieve a water-reducing rate of 30%.

| (**a**) | (**b**) |

Figure 1. (**a**) Basalt fiber. (**b**) Polypropylene fiber.

Table 1. Chemical composition and physical properties of cementitious materials.

Item	OPC	BFS	SF	FA
SiO_2 (%)	21.18	34.65	85.04	35.71
Al_2O_3 (%)	5.02	14.21	0.97	16.57
Fe_2O_3 (%)	3.14	0.49	1.04	8.92
CaO (%)	63.42	34.11	1.63	21.14
MgO (%)	3.12	11.15	0.32	1.41
SO_3 (%)	2.30	1.00	-	1.94
Other	1.82	3.74	10	12.49
Loss of ignition (%)	2.79	0.3	5.48	2.85
Density (g/cm^3)	3.10	2.86	2.1	2.35

Table 2. Physical and mechanical properties of fibers.

Item	Length (mm)	Diameter (μm)	Density (g/cm^3)	Elastic Modulus (GPa)	Tensile Strength (GPa)	Elongation (%)
BF	18	15	2.56	75	4.5	3.15
PF	19	30	0.91	3	0.27	40

2.2. Mix Proportions

The details of all eight mixtures used in this study are presented in Table 3. The eight mixtures had the following fiber contents: 0%, 0.10% (0.05% BF + 0.05% PF), 0.15% (0.05% BF + 0.10% PF), 0.15% (0.10% BF + 0.05% PF), 0.20% (0.05% BF + 0.15% PF), 0.20% (0. 15% BF + 0. 05% PF), 0.20% (0.10% BF+0.10% PF), and 0.30% (0.15% BF + 0.15% PF) (all contents by volume of concrete). These mixtures were termed BF0PF0, BF5PF5, BF5PF10, BF10PF5, BF5PF15, BF15PF5, BF10PF10, and BF15PF15, respectively. For all the mixtures, the water–binder ratio was 0.38 and the concrete constituents excluding the fibers were the same.

Table 3. Mix proportions of concrete (kg/m^3).

| Specimen	OPC	SF	FA	BFS	PBS	Water	Sand	CA	BF	PF
									Volume Fraction (%)	
BF0PF0	241.6	15.8	79.2	59.4	3.96	150.5	683.4	1163.6	0.0	0.0
BF5PF5	241.6	15.8	79.2	59.4	3.96	150.5	683.4	1163.6	0.05	0.05
BF5PF10	241.6	15.8	79.2	59.4	3.96	150.5	683.4	1163.6	0.05	0.10
BF5PF15	241.6	15.8	79.2	59.4	3.96	150.5	683.4	1163.6	0.05	0.15
BF10PF5	241.6	15.8	79.2	59.4	3.96	150.5	683.4	1163.6	0.10	0.05
BF15PF5	241.6	15.8	79.2	59.4	3.96	150.5	683.4	1163.6	0.15	0.05
BF10PF10	241.6	15.8	79.2	59.4	3.96	150.5	683.4	1163.6	0.10	0.10
BF15PF15	241.6	15.8	79.2	59.4	3.96	150.5	683.4	1163.6	0.15	0.15

2.3. Test Method

2.3.1. Mechanical Properties

The compressive strength and splitting tensile strength of all specimens (100 mm × 100 mm × 100 mm) were tested according to GB/T 50081-2002 [35]. The specimens were tested after 28 days of curing under standard curing conditions with a constant temperature of 20 ± 2 °C and a relative humidity greater than 95%. Three specimens of each mixture were tested, and their average value was taken as the final value of the strength.

2.3.2. Pore Structure

The linear traverse method was used to determine the pore characteristic parameters of concrete according to ASTM C 457-9. The pore size distribution of the specimen was measured with a RapidAir 457 air void analyzer (as shown in Figure 2a). Through image recognition, this instrument can measure pore characteristics in hardened concrete by itself, reducing the manual error in testing, and improving measurement speed and accuracy.

(**a**)   (**b**)
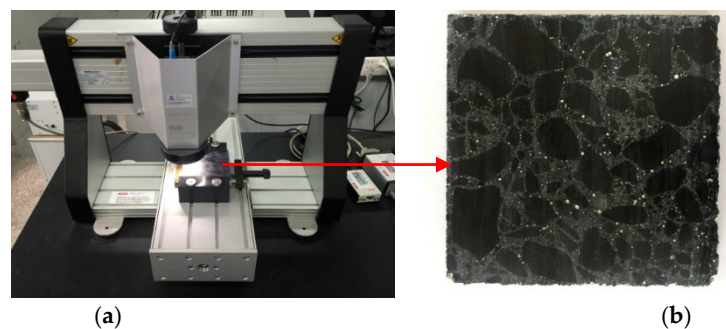
Figure 2. (**a**) Test instrument. (**b**) Test specimen.

The specimens were prepared according to the following procedure. First, all the original specimens were cut after 28 days of standard curing to obtain a specimen with dimensions of 100 mm × 100 mm × 20 mm, without any obvious saw marks on the specimen surface. Second, the specimen was ground with silicon carbide grinding fluid on a lapping machine. Three different grit sizes were used (in the listed order): 320 grit, 600 grit, and 800 grit. Third, the surface of the ground specimen was smeared with carbon black and then zinc paste, and the specimen was heated to 80 °C. When the zinc paste had enough fluidity, it was evenly smeared on the surface of the specimen. Finally, the zinc paste was removed from the specimen surface after cooling. The resultant specimen is shown in Figure 2b.

The test steps are as follows: (1) place the specimen on the sample holder of RapidAir 457 air void analyzer; (2) start the test software, input the basic information of the sample, and make sure that the size of the air voids on the "Analysis Image" have the same size as on the live "Raw Image" by adjusting the focus, lighting and threshold; (3) set the test area of the sample to 80 mm × 80 mm, and then start the test.

3. Fractal Model Based on Optical Method

The contour of the pore section of concrete is complicated and has obvious fractal features. Previous studies have shown that a fractal model based on an optical method is constructed mainly around the solution of the fractal dimension of the pore section contour, e.g., by the perimeter-area method [36]. The fractal model of the concrete pore section is established according to the principle of the perimeter-area method, and the calculation formula is given as follows:

$$\lg P = 0.5 D_p \lg A + C \tag{1}$$

where P is the perimeter, A is the area, D_p is the fractal dimension of pore section contour, C is a constant.

Hu and Tang used the above-described model to study the fractal dimension of concrete [37,38]. Their results demonstrated that the fractal dimension obtained by this model could effectively describe the roughness of concrete, but the correlation between the fractal dimension and the macro-performance of concrete was very low. Therefore, W. Hu improved the model and proposed a new fractal dimension for calculating the pore size distribution [26]; the calculation formula is given as follows:

$$\lg n = D_d \lg d + C \tag{2}$$

where d is the diameter of a pore, n is the number of pores with diameter larger than or equal to d, D_d is the fractal dimension of the pore size distribution, and C is a constant.

The fractal dimension can effectively describe the pore size distribution of concrete by analyzing the experimental data, and it has a good linear relationship with the compressive strength of concrete. According to the test method and the characteristics of the test data, Zhang et al. introduced the box dimension into the previous model. The box dimension is determined by the covering of the same shape set, and it is relatively simple to calculate [39]. The mathematical expression of the box dimension is given as follows: F is an arbitrary nonempty subset of R^n and $N_\delta(F)$ is the minimum number of sets that have a maximum diameter of δ and that can cover set F; then, the box dimension of F can be calculated by formula (3):

$$Dim_B F = \lim_{\delta \to 0} \frac{\lg N_\delta(F)}{\lg(1/\delta)} \tag{3}$$

The pore structure analyzer for hardened concrete measures the number of circular pores at a given circular degree under the assumption that the tested pore in concrete is a regular circular air-hole, and n circular box are selected for measurement according to the definition of the box dimensions. These boxes are used to cover pores whose diameter is greater than or equal to d_i. According to the principle of equal area, the pore with a diameter greater than d_i is transformed into that with the diameter of d_i, and the number of converted pores, N_{ci}, with diameter d_i is obtained. As a result, the data set (d_1, N_{c1}), (d_2, N_{c2}), (d_3, N_{c3}), $\ldots$, (d_i, N_{ci}) is obtained. Finally, data on the pore diameter and the number of converted pores plotted on the double-logarithmic axis are subjected to linear regression analysis, and the slope of the regression line is the box dimension. The corresponding mathematical expression is given in Equation (4):

$$\lg N_c = -D_d \cdot \lg d + C \tag{4}$$

where N_c is the number of converted pores, D_d is the fractal dimension of the pore size distribution, d is the pore diameter, and C is a constant.

4. Experimental Results and Discussion

4.1. Mechanical Properties

The measurement results of the compressive strength and splitting tensile strength of concrete incorporated with mixtures of different fiber contents are shown in Figure 3a,b, respectively. Figure 3a shows that compressive strength can be improved by the incorporation of an appropriate amount of hybrid fibers. The compressive strength of BF5PF5 is the highest, 44.43 MPa, which is 5.06% higher than that of the reference concrete (BF0PF0). However, with an increase in the fiber content, compressive strength becomes lower than that of the reference concrete; BF5PF15 shows the lowest compressive strength, which is 22.63% lower than that of the reference concrete. These findings are in agreement with the results reported by other researchers [40,41]. Sadrinejad et al. demonstrated that the compressive strength and splitting tensile strength of concrete are improved when the content of hybrid fibers was lower than 0.1%, but degraded when the content of hybrid fibers was higher than 0.1% [40]. The incorporation of BF and PF into concrete can reduce microcracks and prevent the expansion of macrocracks, which consequently improves the internal structure of the concrete.

The transverse deformation of concrete under compression is restrained, and the fibers can bond strongly to the matrix. When stress is transferred from the matrix to the fibers, the fibers consume energy because of the deformation, which consequently delays the destruction process of the concrete; as a result, the compressive strength of the concrete improves. However, when the fiber content is too high, the fibers are not uniformly dispersed, and they overlap and agglomerate in the matrix, as shown in Figure 4a; this consequently worsens the bonding effect between the fibers and the matrix [42]. As a result, zones with poor cohesion and weak structures are formed that ultimately nullify the reinforcing effect of the fibers on compressive strength, and this leads to a reduction in compressive strength. Therefore, accurate control of the fiber content of concrete is necessary.

(a)

(b)
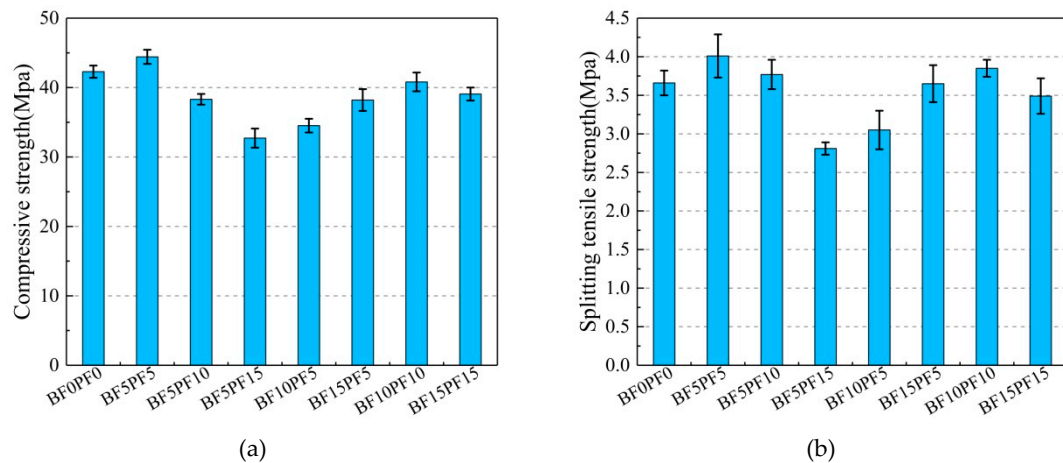
Figure 3. The compressive strength and splitting tensile strength of different mixtures. (**a**) Compressive strength. (**b**) Splitting tensile strength.

(**a**)

(**b**)
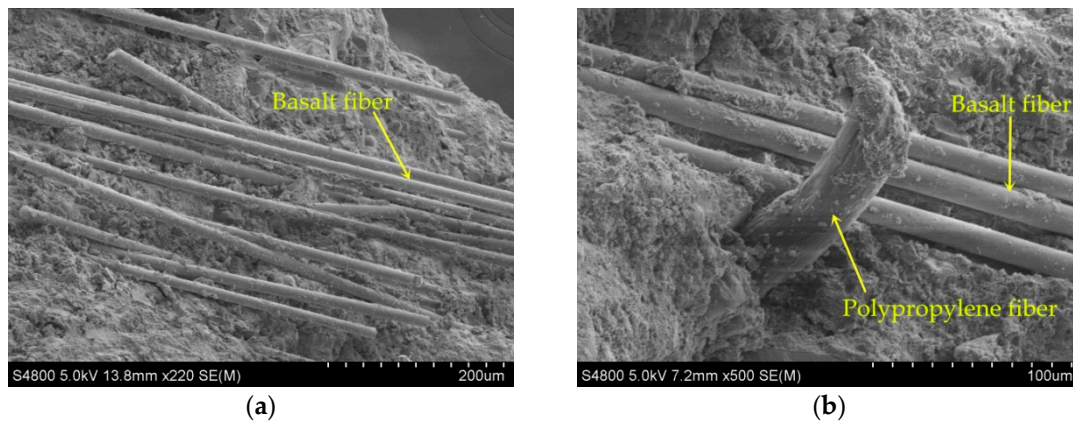
Figure 4. Scanning electron microscopy (SEM) images of fibers. (**a**) Distribution of BF in basalt–polypropylene fiber-reinforced concrete (BPFRC). (**b**) Distribution of BF and PF in BPFRC.

As observed in Figure 3b, the improvement in splitting tensile strength shows a trend similar to that of compressive strength. The test results show that hybrid fibers can effectively improve the splitting tensile strength. The splitting tensile strength of BF5PF5 is the highest, 4.01 MPa, which is 9.56% higher than that of the reference concrete. When the BF content is fixed at 0.05%, splitting tensile strength decreases rapidly with an increasing PF content. BF5PF15 has the lowest splitting tensile strength, which is 23.22% lower than that of the reference concrete. When the content ratio of BF to PF is 1:1, and the total fiber content is higher than 0.2%, the splitting tensile strength is lower than that of the reference concrete. This result is in agreement with previously reported results [4,43]. BF and PF are evenly dispersed or intertwined in the concrete matrix to form a three-dimensional support network, as shown in Figure 4b. When concrete is subjected to loading, the fibers intersect the cracks

transfer the load to the upper and lower surfaces of the cracks, and therefore, the cracks can continue to bear the load. In addition, the fibers can also share part of the tensile force on the section, reduce the stress concentration factor at the micro-cracks in concrete, increase the ultimate tensile strain of concrete, and prevent the formation and propagation of cracks, all of which lead to an improvement in splitting tensile strength. However, when the fiber content is too high, the total surface area of the fibers increases, and a larger amount of cement paste needs to be applied, which adversely affects not only the bonding between the cement paste and the aggregate, but also the splitting tensile strength. The splitting tensile strengths of BF15PF5 and BF10PF10 were higher than that of BF5PF15 when the total fiber content is 0.2%. In general, the results illustrate that the effect of BF on the splitting tensile strength is greater than that of PF [12,14]. This is may be because the elastic modulus and tensile strength of BF are much higher than those of PF. When the microcracks expand further, PFs are pulled out or broken, and then, the tensile stress is borne mainly by the BFs. Therefore, BF plays a major role in the intermediate and later stages of fracture development.

　　Results of the analysis of variance are presented in Table 4, which indicate whether or not there are significant differences in the compressive strength and splitting tensile strength between the BPFRC and reference concrete. According to the significance level of 0.05, when the significance coefficient of BPFRC is less than or equal to 0.05, there is a significant difference in the strength between BPFRC and the reference concrete. Otherwise, there is no significant difference. Therefore, when the BF and PF contents are 0.05% each, the compressive strength and splitting tensile strength are not significantly improved. However, when the fiber contents are (0.05% BF + 0.15% PF) and (0.10% BF + 0.05% PF), the compressive strength and splitting tensile strength are significantly reduced and there is a significant difference between BPFRC and the reference concrete.

Table 4. Compressive strength and splitting tension strength results of different mixtures.

Specimen	Compressive Strength (MPa)			Splitting Tensile Strength (MPa)		
	Mean	SD.	Sig.	Mean	SD.	Sig.
BF0PF0	42.29	0.88	-	3.66	0.16	-
BF5PF5	44.43	1.02	0.066	4.01	0.28	0.199
BF5PF10	38.31	0.77	0.022	3.77	0.19	0.561
BF5PF15	32.72	1.37	0.003	2.81	0.08	0.002
BF10PF5	34.51	0.99	0.009	3.05	0.25	0.045
BF15PF5	38.21	1.57	0.021	3.65	0.24	1.000
BF10PF10	40.81	1.35	0.447	3.85	0.11	0.237
BF15PF15	39.07	0.93	0.113	3.49	0.23	0.441

Mean: the strength of concrete specimen (MPa); SD.: the standard deviations of the measured values; Sig.: the mean difference is significant at the 0.05 level.

4.2. Fractal Dimension of Hardened Concrete

　　The fractal dimension of the pore structure of BPFRC was calculated using the fractal dimension models of Hu [37] and Zhang [39]; the calculation results are shown in Figures 5 and 6, respectively. Figure 5 reveals a good correlation between the logarithmic values of the pore diameter and the number of pores, and the values of the correlation coefficient R^2 of BF5PF10 and BF5PF15 are 0.866 and 0.890, respectively. However, the graph shows an obvious curvilinear relationship, indicating that the model cannot accurately reflect the fractal characteristics of the pore size distribution of BPFRC. Figure 6 shows a double-logarithmic scatter plot of the number of converted pores versus the pore diameter; the figure reveals that the correlation between lgNc and lg$d$ is very high, and the values of the correlation coefficient R^2 of BF5PF10 and BF5PF15 are 0.990 and 0.984, respectively. The graph obtained using Zhang's fractal dimension model shows a more obvious linear relationship than that obtained using Hu's fractal dimension model, which indicates that the fractal features are more obvious when Zhang's model is used and that this model is more reliable. The advantage of Zhang's fractal model is that the definition of the box dimension is used, and the concept of "number of converted

pores" is introduced in the process of constructing the fractal model. Therefore, the fractal dimension calculated using this model is more accurate and reliable, and it can more accurately reflect the fractal characteristics of the pore size distribution. Therefore, in this study, the fractal dimension of BPFRC was calculated using Zhang's fractal model.

The pore structure of concrete can be improved by incorporating fibers into concrete, which affects the fractal dimension of the pore structure [31]. The fractal dimensions of the BPFRC mixtures are listed in Table 5. It can be seen from this table that when the BF content is fixed, the fractal dimension decreases with an increasing PF content; the fractal dimension of BF5PF5 is the largest, 2.482. The fractal dimension of BF5PF15 is the smallest; 7.69% smaller than that of BF5PF5. When the PF content is fixed, the fractal dimension first decreases and then increases with an increasing BF content; the fractal dimension of BF10PF5 is the smallest, 6.16% smaller than that of BF5PF5. The variation in the fractal dimension is very small when the total fiber content is higher than 0.2%.
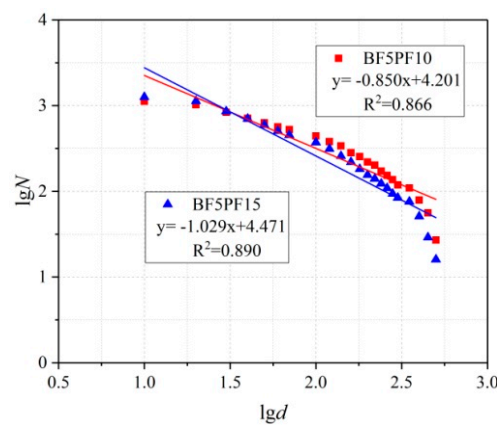

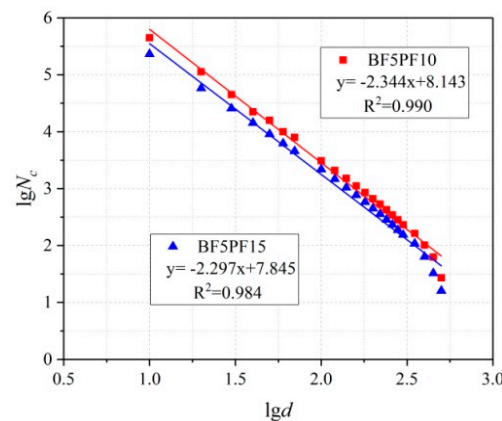**Figure 5.** Double logarithmic scatter plot of cumulative number with pore and pore diameter.

Figure 6. Double logarithmic scatter plot of conversions number with pore and diameter.

Table 5. Results of the fractal dimension.

Specimen	Fractal Dimension	R^2
BF0PF0	2.381	0.979
BF5PF5	2.482	0.977
BF5PF10	2.344	0.990
BF5PF15	2.297	0.984
BF10PF5	2.329	0.986
BF15PF5	2.375	0.980
BF10PF10	2.372	0.982
BF15PF15	2.379	0.977

4.3. Relationship Between Fractal Dimension and Mechanical Properties

The strength of concrete is one of its most important macroscopic performance indexes. The strength is closely related to pore structure parameters such as the air content, porosity and spacing factor [31]. The fractal dimension can synthetically characterize the micropore structure of concrete under certain conditions; therefore, the fractal dimension may have a certain relationship with the strength of concrete [30]. Figure 7 show results of the correlation analysis of the fractal dimension with compressive strength and splitting tensile strength. It can be seen that the fractal dimension has a good correlation with both compressive strength and splitting tensile strength, and the corresponding correlation coefficients are 0.883 and 0.777, respectively. This demonstrates that the fractal dimension as a pore size distribution parameter can well-describe the relationship between pore structure and the mechanical properties of BPFRC. The compressive strength and splitting tensile strength of BPFRC show the same changing trend with an increase in the fractal dimension. That is, compressive strength and splitting tensile strength show an obvious increasing trend with increasing fractal dimension. According to fractal theory, the larger the fractal dimension, the more complex the spatial distribution of pores in concrete and the stronger is the pores' ability to occupy space [44]. Therefore, when the specimens are subjected to stress, the internal stress is distributed evenly, which prevents concentration of premature stress and improves compressive strength and splitting tensile strength; this indicates that the complexity of the pore structure is an important factor affecting the macroscopic performance of concrete. The equation in Figure 7 expresses the relationship between the macroscopic mechanical properties and the micropore structure index and the mode of interaction. This finding is consistent with results reported in the literature [30,31,44].
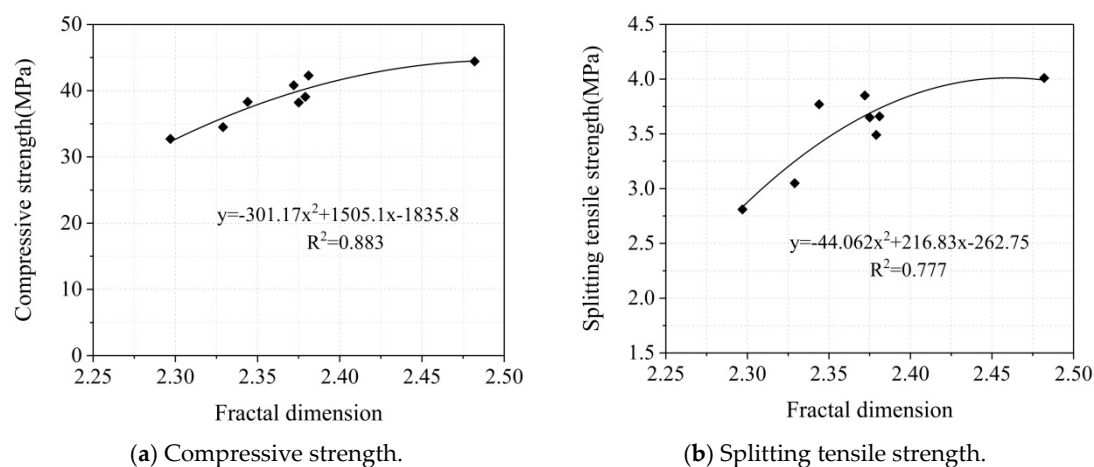

Figure 7. Fitting of strength and fractal dimension.

4.4. Relationship Between Fractal Dimension and Pore Structure Parameters

The variations in the air content and spacing factor of BPFRC with the fractal dimension are shown in Figures 8 and 9, respectively. Air content refers to the ratio of the pore volume in mortar to the total volume of concrete. As can be seen from Figure 8, a good correlation exists between air content and the fractal dimension, and the correlation coefficient is 0.775; air content shows a decreasing trend with increasing fractal dimension. Therefore, under certain conditions, the relative air content can be deduced by a comparison of the fractal dimensions of concrete incorporated with different mixtures. Spacing factor refers to the maximum distance between any point in concrete and any adjacent pore sphere. Figure 9 illustrates the relationship between the fractal dimension and the spacing factor. It can be seen that the spacing factor and fractal dimension also have a good correlation ($R^2 = 0.635$); however, the spacing factor shows an increasing trend with increasing fractal dimension. These results are in agreement with those reported by Liu et al. [45]. It can be noted from our results that a hybrid mixture of BF and PF can improve the pore structure of concrete. When the fractal

dimension increases, the air content decreases whereas the spacing factor increases, which means that both the pore size and the number of pores decrease; that is, the pore structure is refined and optimized. Results of previous works have shown that the air content and spacing factor are the main factors affecting the frost resistance of concrete [46]. Powers also estimated the relationship between the air content and the spacing factor and proposed the critical values of the air content and spacing factor to ensure the frost resistance of concrete [47]. In order to meet the requirement of high frost resistance of concrete, many countries have proposed a recommended value of the air content, which is generally 3–6%; furthermore, studies have recommended that the spacing factor be no larger than 0.25 mm [2]. From the above analysis, it can be seen that the fractal dimension has a strong correlation with the air content and spacing factor, and therefore, the fractal dimension can be used to evaluate pore structure characteristics comprehensively. Therefore, the fractal dimension can be used to predict frost resistance of concrete more effectively.
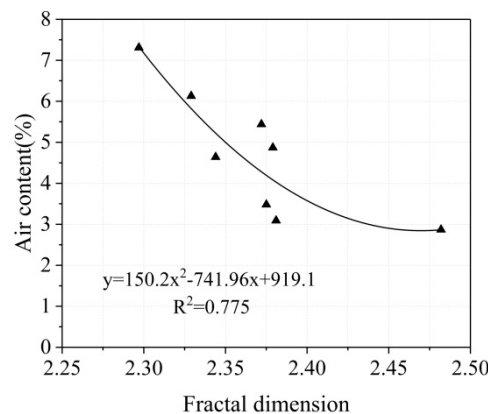

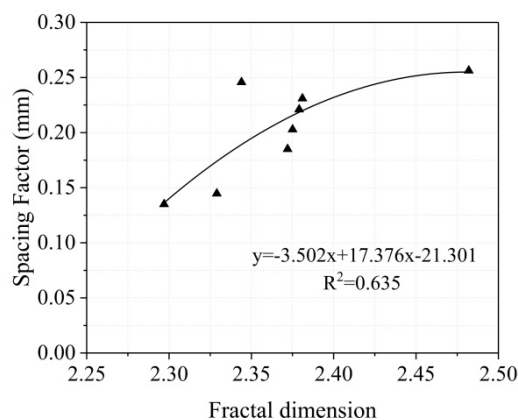**Figure 8.** Fitting of air content and fractal dimension.

Figure 9. Fitting of spacing factor and fractal dimension.

5. Conclusions

In this study, the mechanical properties and pore structure of BPFRC are evaluated. The following conclusions can be drawn from the study.

1. Incorporation of a hybrid mixture of BF and PF into concrete has both positive and adverse effects on the mechanical properties of concrete. The synergistic effect of the hybrid fibers is greatest when the BF and PF contents are 0.05% each; the corresponding increments in the compressive strength and splitting tensile strength 5.06% and 9.56%, respectively. The effect of the hybrid fibers on the splitting tensile strength is greater than that on compressive strength. However, when the fiber content is too high, the hybrid fibers have adverse effects on the mechanical properties. Therefore, accurate control of the fiber content of concrete is necessary.

2. The pore structure of BPFRC exhibits fractal characteristics. The fractal dimension of the pore structure calculated using a fractal model based on an optical method is in the range of 2.297–2.482, with a high correlation coefficient ($R^2 > 0.977$); this indicates that the fractal dimension calculated using this model can well-characterize the pore size distribution characteristics of concrete.

3. The fractal dimension of BPFRC is closely related to the air content and spacing factor. As the fractal dimension increases, the air content decreases and the spacing factor increases. Therefore, the pore structure characteristics of BPFRC can be evaluated comprehensively using the fractal dimension. In addition, the fractal dimension has a strong positive correlation with the compressive strength and splitting tensile strength of concrete. That is, the larger the fractal dimension, the higher the compressive strength and splitting tensile strength. This indicates that the complexity of the pore structure is an important factor affecting the macroscopic mechanical properties of concrete.

Author Contributions: D.N. and D.H. conceived the main concept and contributed the analysis; D.H., L.S., and H.Z. conducted experiments; Q.F. and D.L. helped analyzing experimental data; D.H. wrote the paper.

Conflicts of Interest: The authors declare no conflict of interest.

References

1. Jin, W.L.; Zhao, Y.X. *Durability of Concrete Structures*, 2nd ed.; Science Press: Beijing, China, 2014; pp. 13–17.
2. Li, Y.; Zhao, W. *Resistance Crack Toughening and Durability of Hybrid Fiber Concrete*, 1st ed.; Science Press: Beijing, China, 2012; pp. 1–6.
3. Xue, M.K. Research of Mechanical Properties for Basalt and Polypropylene Mixed Fiber Concrete. Master's Thesis, Anhui University of Science and Technology, Huainan, China, 2018.
4. Ghazy, A.; Bassuoni, M.T.; Maguire, E.; Oloan, M. Properties of Fiber-Reinforced Mortars Incorporating Nano-Silica. *Fibers* **2016**, *4*, 6. [CrossRef]
5. Afroughsabet, V.; Biolzi, L.; Ozbakkaloglu, T. High-Performance Fiber-Reinforced Concrete: A Review. *J. Mater. Sci.* **2016**, *51*, 6517–6551. [CrossRef]
6. Tadepalli, P.R.; Mo, Y.L.; Hsu, T.T.C. Mechanical Properties of Steel Fibre Concrete. *Mag. Concr. Res.* **2013**, *65*, 462–474. [CrossRef]
7. Sun, Z.Z.; Xu, Q.W. Microscopic, Physical and Mechanical Analysis of Polypropylene Fiber Reinforced Concrete. *Mater. Sci. Eng. A* **2009**, *527*, 198–204. [CrossRef]
8. Badogiannis, E.G.; Christidis, K.I.; Tzanetatos, G.E. Evaluation of the Mechanical Behavior of Pumice Lightweight Concrete Reinforced with Steel and Polypropylene Fibers. *Constr. Build. Mater.* **2019**, *196*, 443–456. [CrossRef]
9. Pajak, M. Investigation on Flexural Properties of Hybrid Fibre Reinforced Self-Compacting Concrete. *Procedia Eng.* **2016**, *161*, 121–126. [CrossRef]
10. Aslani, F.; Nejadi, S. Self-Compacting Concrete Incorporating Steel and Polypropylene Fibers: Compressive and Tensile Strengths, Moduli of Elasticity and Rupture, Compressive Stress-Strain Curve, and Energy Dissipated Under Compression. *Compos. Part B Eng.* **2013**, *53*, 121–133. [CrossRef]
11. Li, C.R.; Wang, X.Z.; Liu, H.X.; Hu, K.X.; Li, G. Research Progress of Hybrid Fiber Reinforced Concrete. *J. Mater. Sci Eng.* **2018**, *36*, 504–510.
12. Jiang, C.H.; Fan, K.; Wu, F.; Chen, D. Experimental Study on the Mechanical Properties and Microstructure of Chopped Basalt Fibre Reinforced Concrete. *Mater. Des.* **2014**, *58*, 187–193.
13. Fiore, V.; Scalici, T.; Bella, G.D.; Valenza, A. A Review on Basalt Fibre and its Composites. *Compos. Part B Eng.* **2015**, *74*, 74–94. [CrossRef]
14. Wang, D.H.; Ju, Y.Z.; Shen, H.; Xu, L.B. Mechanical Properties of High Performance Concrete Reinforced with Basalt Fiber and Polypropylene Fiber. *Constr. Build. Mater.* **2019**, *197*, 464–473. [CrossRef]

15. Kong, X.Q.; Yuan, S.L.; Dong, J.K.; Gang, J.M.; Zhang, W.J. Experimental Study on Performance of Polypropylene-Basalt Hybrid Fiber Reinforced Recycled Aggregate Concrete after Exposure to Elevated Temperatures. *Sci. Technol. Eng.* **2018**, *18*, 101–106.

16. Zhao, B.B.; He, J.J.; Wang, X.Z.; Zheng, S.W. Experimental Study on Mechanical Properties of Concrete with Basalt-Polypropylene Hybrid Fiber. *China Concr. Cem. Prod.* **2014**, *8*, 51–55.

17. He, J.J.; Shi, J.P.; Wang, X.Z.; Han, T.L. Effect of Hybrid Effect on the Mechanical Properties of Hybrid Fiber Reinforced Concrete. *Fiber Reinf Plast Compos.* **2016**, *9*, 26–31.

18. Wu, P.; Wang, J.; Wang, X.Y. A Critical Review of the Use of 3-D Printing in the Construction Industry. *Autom. Constr.* **2016**, *68*, 21–31. [CrossRef]

19. Christ, S.; Schnabel, M.; Vorndran, E.; Groll, J.; Gbureck, U. Fiber Reinforcement during 3D Printing. *Mater. Lett.* **2015**, *139*, 165–168. [CrossRef]

20. Hambach, M.; Volkmer, D. Properties of 3D-Printed Fiber-Reinforced Portland Cement Paste. *Cem. Concr. Compos.* **2017**, *79*, 62–70. [CrossRef]

21. Panda, B.; Paul, S.C.; Tan, M.J. Anisotropic Mechanical Performance of 3D Printed Fiber Reinforced Sustainable Construction Material. *Mater. Lett.* **2018**, *184*, 1005–1010. [CrossRef]

22. Ma, G.W.; Li, Z.J.; Wang, L.; Wang, F.; Sanjayan, J. Mechanical Anisotropy of Aligned Fiber Reinforced Composite for Extrusion-Based 3D Printing. *Constr. Build. Mater.* **2019**, *202*, 770–783. [CrossRef]

23. Yousfi, A.; Fréour, S.; Jacquemin, F. Eshelby-Kröner Viscoelastic Self-Consistent Model: Multi-Scale Behavior of Polymer Composites Under Creep Loading. *Adv. Mater. Res.* **2013**, *682*, 105–112. [CrossRef]

24. Xiao, J.H.; Xu, Y.L.; Zhang, F.C. A Generalized Self-Consistent Method for Nano Composites Accounting for Fiber Section Shape under Antiplane Shear. *Mech. Mater.* **2015**, *81*, 94–100. [CrossRef]

25. Mori, T.; Tanaka, K. Average Stress in Matrix and Average Elastic Energy of Materials with Misfitting Inclusions. *Acta Metall.* **1973**, *21*, 571–574. [CrossRef]

26. Lukkassen, D.; Persson, L.-E.; Wall, P. Some Engineering and Mathematical Aspects on the Homogenization Method. *Compos. Eng.* **1995**, *5*, 519–531. [CrossRef]

27. Cai, Y.W. Asymptotic Homogenization of Periodic Plate and Micro-Structural Optimization. Ph.D. Thesis, Dalian University of Technology, Dalian, China, 2014.

28. Lian, C.; Zhuge, Y.; Beecham, S. The Relationship between Porosity and Strength for Porous Concrete. *Constr. Build. Mater.* **2011**, *25*, 4294–4298. [CrossRef]

29. Arandigoyen, M.; Alvarze, J.I. Pore structure and Mechanical Properties of Cement–Lime Mortars. *Cem. Concr. Res.* **2007**, *37*, 767–775. [CrossRef]

30. Jin, S.S.; Zhang, J.X.; Han, S. Fractal Analysis of Relation between Strength and Pore Structure of Hardened Mortal. *Constr. Build. Mater.* **2017**, *135*, 1–7. [CrossRef]

31. Cui, S.A.; Liu, P.; Cui, E.Q.; Su, J.; Huang, B. Experimental Study on Mechanical Property and Pore Structure of Concrete for Shotcrete use in a Hot-Dry Environment of High Geothermal Tunnels. *Constr. Build. Mater.* **2018**, *173*, 124–135. [CrossRef]

32. Zhao, Y.R.; Guo, Z.L.; Fan, X.Q.; Shi, J.N.; Wang, L. Basalt Fiber Reinforced Concrete Stress-Strain Relationship and Pore Structure Analysis. *Bull. Chin. Ceram. Soc.* **2017**, *36*, 4142–4150.

33. Yu, L.H.; Ou, H.; Duan, Q.P. Research on Pore Volume Fractal Dimension and its Relation to Pore Structure and Strength in Cement Paste with Perlite Admixture. *J. Mater. Sci. Eng.* **2007**, *25*, 201–204.

34. Ji, X.; Chan, S.Y.N.; Feng, N. Fractal Model for Simulating the Space-Filling Process of Cement Hydrates and Fractal Dimensions of Pore Structure of Cement-Based Materials. *Cem. Concr. Res.* **1997**, *27*, 1691–1699. [CrossRef]

35. Chinese National Standards. *GB/T 50081-2002, Standard for Method of Mechanical Properties on Ordinary Concrete*, 1st ed.; China Architecture and Building Press: Beijing, China, 2003; pp. 12–24.

36. Chu, W.Y. *Fractals in Materials Science*, 1st ed.; Chemical Industry Press: Beijing, China, 2004; pp. 3–32.

37. Hu, W. Modeling the Influence of Composition and Pore Structure on Mechanical Properties of Autoclaved Cellular Concrete. Ph.D. Thesis, University of Pittsburgh, Pittsburgh, PA, USA, 1997.

38. Tang, M. Study on Fractal Characteristics and Application of Concrete Materials. Ph.D. Thesis, Harbin Institute of Technology, Harbin, China, 2003.

39. Zhang, J.X.; Jin, S.S. *Micropore Structure of Cement Concrete and Its Function*, 1st ed.; Science Press: Beijing, China, 2014; pp. 34–44.

40. Sadrinejad, I.; Madandoust, R.; Ranjbar, M.M. The Mechanical and Durability Properties of Concrete Containing Hybrid Synthetic Fibers. *Constr. Build. Mater.* **2018**, *178*, 72–82. [CrossRef]

41. Liu, D.C. Study on the Properties of Basalt and Polypropylene Mixed Fiber Concrete. Master's Thesis, Chongqing Jiaotong University, Chongqing, China, 2018.

42. Mydin, M.A.O.; Soleimanzadeh, S. Effect of Polypropylene Fiber Content on Flexural Strength of Lightweight Foamed Concrete at Ambient and Elevated Temperatures. *Adv. Appl. Sci. Res.* **2012**, *3*, 2837–2846.

43. Yap, S.P.; Alengaram, U.J.; Jumaat, M.Z. Enhancement of Mechanical Properties in Polypropylene-and Nylon-Fibre Reinforced Oil Palm Shell Concrete. *Mater. Des.* **2013**, *49*, 1034–1041. [CrossRef]

44. Li, Y.X.; Chen, Y.M.; He, X.Y. Pore Volume Fractal Dimension of Fly Ash-Cement Paste and its Relationship between the Pore Structure and Strength. *J. Chin. Ceram. Soc.* **2003**, *31*, 774–779.

45. Liu, H.Y.; Li, H.Y.; Zou, C.X. Effect of Fiber Elastic Modulus on Concrete Bubble Fractal Dimension and Frost Durability of Light-Weight Aggregate Concrete. *Bull. Chin. Ceram. Soc.* **2015**, *34*, 3039–3044.

46. Shi, Y.; Yang, H.Q.; Chen, X.; Li, X.; Zhou, S.H. Influence of Aggregate Variety on Pore Structure and Microscopic Interface of Concrete. *J. Build. Mater.* **2015**, *18*, 133–138.

47. Powers, T.C. Void Spacing as a Basis for Producing Air-Entrained Concrete. *J. Am. Concr. Inst.* **1954**, *50*, 741–759.